ORGANIC LETTERS

2011
Vol. 13, No. 5
1198–1201

Hammett Analysis of a Family of Carbene−Carbene Complex Equilibria†

Lei Wang, Robert A. Moss,* Jack Thompson,‡ and Karsten Krogh-Jespersen*

Department of Chemistry and Chemical Biology, Rutgers, The State University of New Jersey, New Brunswick, New Jersey 08903, United States

moss@rutchem.rutgers.edu; krogh@rutchem.rutgers.edu

Received January 11, 2011

ABSTRACT

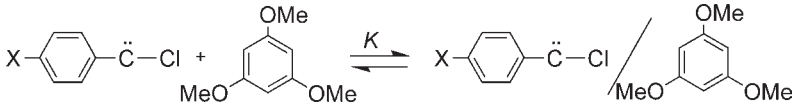

***p*-X-substituted phenylchlorocarbenes (X = NO_2, CF_3, Cl, H, Me, and MeO) form π-type complexes with trimethoxybenzene in pentane. The carbenes and complexes are in equilibrium, and logarithms of the measured equilibrium constants are well correlated by Hammett σ_p constants with ρ = 2.48. The carbene complexes are characterized by UV−vis spectroscopy, and computational analysis is afforded by DFT calculations.**

We recently provided the first direct spectroscopic evidence for a carbene−carbene complex equilibrium, eq 1.[1,2] Phenylchlorocarbene (**1d**), generated by laser flash photolysis (LFP) of phenylchlorodiazirine, formed π-type complexes ($\tau \sim 500$ ns) with 1,3,5-trimethoxybenzene (TMB) in pentane. From the UV−vis absorptions of carbene **1d** and complex(es) **2d** as a function of TMB concentration, we determined K = 1264 M^{-1} at 294 K.

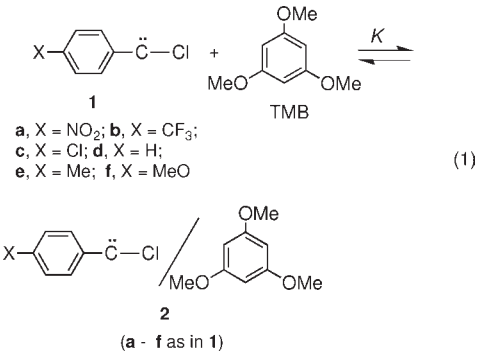

a, X = NO_2; **b**, X = CF_3; **c**, X = Cl; **d**, X = H; **e**, X = Me; **f**, X = MeO

(1)

Here, we document equilibria within a *family* of *p*-substituted phenylchlorocarbenes, **1a**−**1f**, and their respective complexes with TMB, **2a**−**2f**, where the *para* substituents are NO_2, CF_3, Cl, H, Me, or MeO. The measured equilibrium constants (K at 294 K) range from a high of 1.34×10^5 M^{-1} for **1a** (X = NO_2) to a low of 164 M^{-1} for **1f** (X = MeO). The values of K are well correlated by the Hammett equation (log K vs σ_p) with ρ = 2.48.

p-X-Substituted phenylchlorodiazirines **3b**−**3f** were prepared by Graham oxidation[3] of benzamidine hydrochlorides **4b**−**4f**, which are described in the literature.[4] Detailed procedures for the preparation of diazirine **3a** were published more recently.[5] UV spectra of diazirines **3a**−**3f** appear in the Supporting Information.

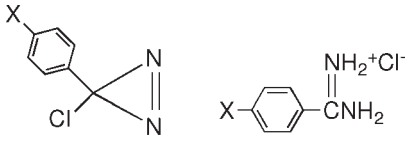

(**a** - **f** as in **1**)

LFP[6] of diazirines **3a**−**3f** in pentane afforded carbenes **1a**−**1f**, which displayed strong π(Ph) → p(carbene) absorptions between 308 and 324 nm and weak σ(carbene) → p(carbene) absorptions between 588 and 676 nm.[7,8] In the

† Dedicated to Professor Ronald Breslow on the occasion of his 80th birthday.

‡ Undergraduate exchange student from The University of Manchester, Manchester, England.

(1) Moss, R. A.; Wang, L.; Odorisio, C. M.; Krogh-Jespersen, K. *J. Am. Chem. Soc.* **2010**, *132*, 10677.

(2) For other examples of carbene complexes, see: (a) Tippmann, E. M.; Platz, M. S.; Svir, I. B.; Klymenko, O. V. *J. Am. Chem. Soc.* **2004**, *126*, 5750. (b) Wang, J.; Kubicki, J.; Peng, H.; Platz, M. S. *J. Am. Chem. Soc.* **2008**, *130*, 6604.

(3) Graham, W. H. *J. Am. Chem. Soc.* **1965**, *87*, 4396.

(4) Moss, R. A.; Terpinski, J.; Cox, D. P.; Denney, D. Z.; Krogh-Jespersen, K. *J. Am. Chem. Soc.* **1985**, *107*, 2743. Full experimental details for the benzamidine preparations appear in this publication.

(5) Moss, R. A.; Wang, L.; Weintraub, E.; Krogh-Jespersen, K. *J. Phys. Chem. A* **2008**, *112*, 4651.

(6) We used a XeF_2 excimer laser emitting 14 ns light pulses at 351 nm with 55−65 mJ power. For more details, see: Moss, R. A.; Tian, J.; Sauers, R. R.; Ess, D. H.; Houk, K. N.; Krogh-Jespersen, K. *J. Am. Chem. Soc.* **2007**, *129*, 5167.

10.1021/ol200083a
Published on Web 02/10/2011

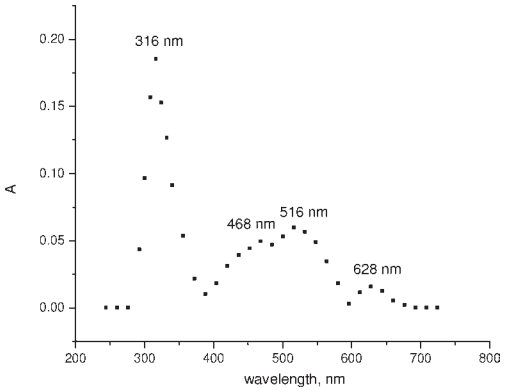

Figure 1. UV−vis spectra of carbene **1a** and its TMB complex(es) (**2a**) in 0.011 mM TMB in pentane: **1a** absorptions at 316 and 628 nm; **2a** absorptions at 468 and 516 nm.

presence of TMB, new absorptions appeared due to the formation of carbene complexes **2a**−**2f**. The intensities of the carbene complex absorptions grew as the concentration of TMB was increased, with concomitant diminution in the intensities of the associated carbene absorptions. An example of the calibrated[9] carbene plus carbene complex spectra for the *p*-NO_2 (**1a**/**2a**) system appears in Figure 1; complete sets of calibrated spectra for all carbenes and their complexes at various TMB concentrations are collected in the Supporting Information.[10]

Table 1. Absorption Maxima of Carbenes and Complexes

carbene	λ_{max} (nm)[a]	complex	λ_{max} (nm)[b]
1a	316, 628	**2a**	468, 516
1b	308, 628	**2b**	404, 500
1c	324, 650	**2c**	436, 500
1d[c]	308, 588	**2d**[c]	484, 596
1e	316, 644	**2e**	404, 484
1f	324, 676	**2f**	436, 492

[a] In pentane. [b] In pentane and TMB. [c] From ref 1.

Table 1 records the observed absorption maxima of carbenes **1a**−**1f** and complexes **2a**−**2f**; computational analysis (see below) helps us assign the TMB-induced absorptions to specific ArCCl/TMB complexes. Figure 2 illustrates the two dominant π-complexes computed for the **1e**/TMB complexes (X = Me); similar structures are computed for the other carbene/TMB complexes.[1] The

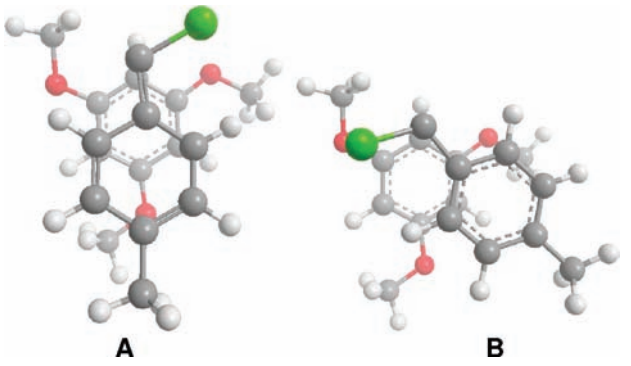

Figure 2. Two computed complexes formed between carbene **1e** (X = Me) and TMB (in perspective and with depth fading, carbene on top; green chlorine; red oxygen). Computed absorptions are (**A**) 437 nm and (**B**) 465 nm; the corresponding observed absorptions are at 404 and 484 nm.

formation of complexes **2a**-**2f** is calculated to be enthalpically favorable in all cases; further discussion of the carbene complex structures and energetics appears below.

Although the **2a**−**2f** complexes are computed to also absorb in the 308−324 nm region where the carbenes have their principal absorptions (Table 1), it is possible to quantitatively evaluate the contribution of the carbenes alone in the UV−vis spectra of the mixtures of carbenes and carbene complexes.[1] The analysis substitutes *computed* oscillator strengths (*f*) for the requisite but experimentally unknown extinction coefficients of the carbenes and their complexes; see the Supporting Information for details. We are thus able to evaluate *K* for the equilibrium of eq 1 for each of the six carbene−carbene complex systems.

As an example, consider **1c**/**2c** (X = Cl). A plot of the quotient of the calibrated intensities of the 312 nm (**1c** + **2c**) and 500 nm (**2c**) absorptions versus 1/[TMB] affords the linear correlation of Figure 3, where the slope (8.62×10^{-4} M) leads to $K = 5440\ M^{-1}$ for eq 1.[11]

In a similar manner, *K* was determined for the other carbene−carbene complex systems. Details of these equilibrium constant measurements appear in the Supporting Information. Table 2 collects the *K* values, their logarithms, and the appropriate Hammett σ_p constants.[12] Note that these *K* values are associated with carbene complexes of type **B** (see Figure 2), because the complex absorption of lowest energy was monitored.[13]

A good Hammett correlation of log *K* versus σ_p appears in Figure 4, where $\rho = 2.48$ and $r = 0.990$. The positive sign associated with ρ means that the complexation in eq 1

(7) The $\sigma \rightarrow$ p absorption of **1d** appears at 588 nm.[1,8]

(8) Pliego, J. R., Jr.; De Almeida, W. B.; Celebi, S.; Zhu, Z.; Platz, M. S. *J. Phys. Chem. A* **1999**, *103*, 7481.

(9) Calibration corrects the raw UV−vis absorptions for wavelength-dependent variations in sample absorptivity, xenon monitoring lamp emission, and detector sensitivity.[1] Calibration spectra are collected in the Supporting Information.

(10) The spectra for carbene **1d** (X = H) and its TMB complexes appear in ref 1 and its Supporting Information.

(11) $K = (1/\text{slope})(f_3/f_1)$, where f_3 (0.493) is the computed oscillator strength of carbene **1c** at 310 nm and f_1 (0.105) is the computed oscillator strength for complex **2c** at 483 nm (assigned to the observed absorption at 500 nm). See the Supporting Information for details.

(12) Smith, M. B.; March, J. *March's Advanced Organic Chemistry*, 6th ed.; Wiley Interscience: Hoboken, NJ, 2007; p 404.

(13) The absorptions used to calculate *K* are those corresponding to the computed absorptions for the **B**-type complexes of Figure 2. The observed absorptions assigned to the **A**-type complexes overlap significantly with the "**B**" absorptions and cannot be separately evaluated; cf. the absorption spectra in the Supporting Information.

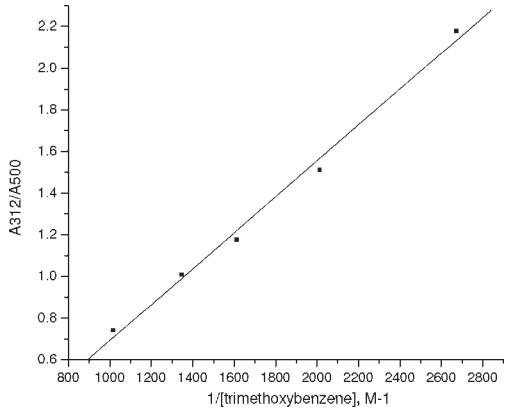

Figure 3. Relative absorption intensities at 312 nm/500 nm versus 1/[TMB] for carbene **1c** in pentane/TMB solution at 294 K. The slope of the correlation line is 8.62×10^{-4} M ($r = 0.997$), leading to $K = 5440$ M^{-1} for eq 1.[11]

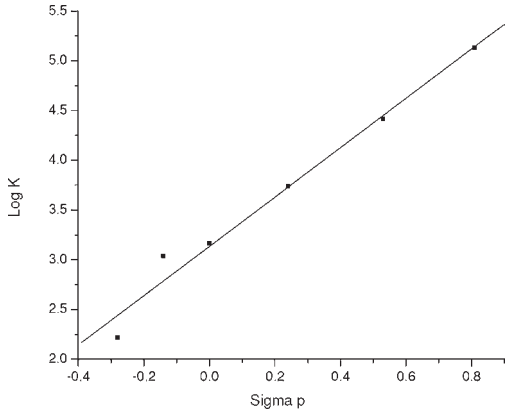

Figure 4. Hammett correlation of log K versus σ_p for the experimental data of Table 2; $\rho = 2.48$, $r = 0.990$.

Table 2. Equilibrium Constants for Equation 1

carbene (X)	K (M^{-1})[a]	log K[a]	σ_p[b]
1a (NO_2)	134,000	5.13	0.81
1b (CF_3)	25,800	4.41	0.53
1c (Cl)	5,440	3.74	0.24
1d (H)	1,450[c]	3.16	0.00
1e (Me)	1,080	3.03	−0.14
1f (OMe)	164	2.21	−0.28

[a] Shown to 3 significant figures. [b] From ref 12. [c] This value differs from K given in ref 1 (1260 M^{-1}) because here only the computed f value for the **B**-type complex is used to calculate K. In ref 1 we used an average of the f values computed for the **A**- and **B**-type complexes.

is favored by substitution of electron-withdrawing substituents on carbenes **1a**−**1f**.[12] The magnitude of ρ obtained here is similar to that established for the dissociation equilibria of ArOH in water (2.11), ArSH in 49% ethanol (2.24), $ArNH_3^+$ in water (2.77), and ArCOOH in ethanol (2.28).[14]

Qualitatively, we can interpret the positive ρ in two complementary ways: (1) electron-withdrawing groups destabilize carbenes **1a**−**1f**,[15] shifting the equilibrium toward complexes **2a**−**2f** where TMB donates electron density to the vacant carbenic p orbital (viz. Figure 2); (2) stronger π-type charge transfer complexes **2a**−**2f** will be formed when the electron-rich TMB interacts with the more electron-deficient carbene center/aromatic ring induced by an electron-withdrawing substituent.

Electronic structure calculations based on density functional theory provide structures and energetics of potential **2a**−**2f** complexes (B97D/6-311+G(d), data in Table 3) and predict electronic absorption frequencies and intensities (B3LYP/6-311+G(d)//B97D/6-311+G(d)).[16] We have previously shown that density functionals such as B97D, which explicitly include dispersion corrections, provide appropriate binding energies of PhCCl/TMB complexes.[1] We also found that sandwich-type structures, in which the π-systems of the aromatic ring moieties overlap significantly, formed the most stable complexes (viz. **A** and **B** in Figure 2). In both types of complexes, the binding enthalpies are substantial, ΔH° ranges from −15.5 kcal/mol (**2a**, **A**) to −9.5 kcal/mol (**2f**, **B**) (see Table 3), and the carbene carbon interacts strongly with the unsubstituted C2 carbon of TMB. Computed C(carbene)−C2(TMB) distances (r) span the range 2.7−3.0 Å in type **A** complexes and 2.9−3.1 Å in type **B** complexes (Table 3). Within each type of

Table 3. Thermodynamic Parameters for *p*-X-PhCCl/TMB Complexes **2a**−**2f**: Enthalpy (ΔH°), Entropy (ΔS°), and Gibbs Free Energy (ΔG°) Changes and Equilibrium Constants (K) Computed at the B97D/6-311+G(d) Level

complex	r[a]	ΔH°[b]	ΔS°[b,c]	ΔG°[b]	$\Delta\Delta G^\circ$	K[c]	K_{rel}
			A-type				
2a (NO_2)	2.66	−15.5	−38.5	−4.0	−3.1	877	181
2b (CF_3)	2.71	−14.1	−38.0	−2.8	−1.9	113	23
2c (Cl)	2.82	−12.3	−35.3	−1.8	−0.9	20	4.2
2d (H)	2.81	−11.0	−33.7	−0.9	0.0	4.8	1.0
2e (Me)	2.87	−11.1	−36.2	−0.3	0.7	1.6	0.3
2f (OMe)	2.99	−10.8	−34.1	−0.6	0.3	2.8	0.6
			B-type				
2a (NO_2)	2.88	−13.4	−37.8	−2.2	−2.6	40	80
2b (CF_3)	2.93	−12.8	−38.3	−1.3	−1.7	9.5	19
2c (Cl)	3.00	−11.0	−35.1	−0.5	−0.9	2.3	4.6
2d (H)	2.96	−10.0	−35.0	0.4	0.0	0.5	1.0
2e (Me)	3.02	−9.8	−34.6	0.5	0.1	0.4	0.9
2f (OMe)	3.11	−9.5	−33.5	0.5	0.1	0.4	0.8

[a] C(carbene)−C2(TMB) distance, in Å. [b] ΔH° and ΔG° in kcal/mol, ΔS° in eu, relative to the separated reactants; $T = 298.15$ K. ΔG° and ΔS° computed using a reference state of 1 M concentration for each species participating in the reaction. [c] Units are M^{-1}.

(14) (a) Jaffe, H. H. *Chem. Rev.* **1953**, *53*, 191. (b) Wells, P. R. *Chem. Rev.* **1963**, *63*, 171.

(15) Rondan, N. G.; Houk, K. N.; Moss, R. A. *J. Am. Chem. Soc.* **1980**, *102*, 1770.

complex we generally find that as the carbene−TMB interaction distance decreases, the binding enthalpy increases. In type **A** complexes, the carbenic Cl atom points toward the open back-side of an adjacent MeO group and does not appear to be sterically encumbered. In type **B** complexes, the Cl atom is situated above an adjacent oxygen atom and is sterically encumbered by the MeO group. As illustrated in Figure 2, the Cl−MeO steric interaction forces the aromatic rings in Type **B** complexes to rotate relative to each other, and consequently, there is more stabilizing face-to-face ring overlap in complexes of type **A**. For a particular *para* substituent (X), the **A** − **B** energy difference is 1−2 kcal/mol (Table 3).

The entropy changes associated with complex formation ($\Delta S^{o} \approx -35$ eu, Table 3) are overestimated by the electronic structure calculations, which refer to idealized gas phase rather than solution phase conditions. Thus, despite the very favorable complexation enthalpies obtained at the B97D/6-311+G(d) level, the computed Gibbs free energies of complexation are too large, and the computed equilibrium constants are consequently smaller than the experimentally derived quantities. Unquestionably, electron-withdrawing groups (NO_2, CF_3, and Cl) in the *p*-position lead to more favorable free energies of complexation (larger *K*), and electron-donating groups (Me and MeO) disfavor complex formation. The relative magnitudes of the substituent effects appear to be reproduced much better for the electron-withdrawing groups than for the electron-donating groups; in particular, the destabilizing effect of MeO is seriously underestimated by the calculations.[17] Nevertheless, a plot of the Gibbs free energy changes, or equivalently, a logarithmic plot of the equilibrium constants versus the Hammett substituent parameters, displays a reasonable straight line. For the **B** complexes, the slope $\rho = 1.95$ ($r = 0.982$) is in satisfactory agreement with the experimentally defined value of 2.48 (Figure 4); for the **A** complexes $\rho = 2.49$ ($r = 0.979$).[13] These Hammett correlation diagrams appear in the Supporting Information.

p-X-PhCCl/TMB complex formation is accompanied by the appearance of an electronic absorption band in the 400−500 nm region. The new band embodies considerable π(HOMO, TMB) → p(LUMO, carbene) charge transfer character, although neither experimental (Table 1) or computed (Table S-1 in Supporting Information) band maxima shift in a systematic manner as the *para* substituent (X) changes. For a particular substituent, the **B** complex absorbs at lower energy with a smaller oscillator strength than the **A** complex (Table S-1), qualitatively in accord with the lesser overlap and interaction between the aryl rings present in the **B** complexes (Figure 2). In the experimental spectra, we therefore associate the higher-energy band with the **A**-type complexes and the lower-energy band with the **B**-type complexes. Flanking these signature bands are mixed absorption bands reflecting the coexistence of free carbenes and carbene complexes in solution.

The experimental spectra appear to show larger intensities in the low-energy bands, which we ascribe to **B**-type complex formation, than in the high-energy bands (**A**-type complexes). In contrast, the calculations predict that a carbene/TMB solution mixture at equilibrium should contain more complexes of type **A** than of type **B** (Table 3); furthermore, the signature transition of complex formation is predicted to carry larger intensity in the **A**-type complexes (Table S-1). The electronic structure calculations locate the single most stable carbene/TMB configuration on the potential energy surface in an idealized gas phase. It is plausible that on the "solution free energy surface" complexes of the less geometrically restricted **B**-type actually dominate, so that the absorption toward the red appears more intense in the experimental spectra as a result of a larger equilibrium concentration of complexes.

In summary, using a combination of LFP and DFT techniques, we have determined equilibrium constants for a family of *p*-substituted phenylchlorocarbene/TMB complexes. The substituent effects on the experimental and computational equilibrium constants are well correlated by the Hammett equation.

Acknowledgment. We are grateful to the National Science Foundation for financial support.

Supporting Information Available. Figures S-1−S-51, Table S-1, computational details, and optimized geometries, absolute energies, electronic excitation energies and oscillator strengths of all relevant species. This material is available free of charge via the Internet at http://pubs.acs.org.

(16) All calculations made use of the Gaussian 09, Revision A02 program package: Frisch, M. J. et al. . Gaussian, Inc.: Wallingford, CT, 2009; see Supporting Information for additional computational details and the complete reference for Gaussian 09.

(17) It was necessary to tighten the geometry optimization criteria and to increase the size of the integration grid relative to their default values to reach even this level of agreement and consistency. Test calculations with larger basis sets and/or different dispersion-corrected functionals did not show any improvement for X = MeO.